NONLINEAR RELATIVE RADIOMETRIC NORMALIZATION FOR LANDSAT 7 AND LANDSAT 8 IMAGERY

Lino Garda Denaro (1), Chao Hung Lin (1)

[1] Geospatial Artificial Intelligence Laboratory, Geomatics Department, National Cheng Kung University, 1 University Road, 70101, Tainan City, Taiwan, R.O.C.
Email: dgarda.lino@gmail.com; linhung@mail.ncku.edu.tw

KEY WORDS: Relative radiometric normalization, pseudo-invariant features, kernel canonical correlation analysis, nonlinear regression.

ABSTRACT: Relative radiometric normalization (RRN) minimizes radiometric differences among images caused by inconsistencies of acquisition condition. In this study, a cross-sensor RRN method is proposed for optical satellite images from Landsat 8 OLI (L8) and Landsat 7 ETM+ (L7) sensors. The data from these two sensors have different pixel depths. Therefore, a rescaling on the radiometry resolution is performed in the preprocessing. Then, multivariate alteration detection (MAD) based on kernel canonical correlation analysis (KCCA) is adopted, which is called KCCA-based MAD, to select pseudo-invariant features (PIFs). The process of RRN is performed by using hybrid linear, power-law and polynomial regression with Gaussian weighted regression. In experiments, qualitative and quantitative analyses on images from different sensors are conducted. The experimental result demonstrates the superiority of the proposed nonlinear transformation, in terms of regression quality and radiometric consistency, compared with RRN using linear regression.

1. INTRODUCTION

Earth spatial diversity commonly can be measured by the remote sensing strategy (D. Yuan et al., 1996). The analyzation of the spatial diversity mainly reached with the retrieval of the images that are captured by the satellites at different time and distances. Each of captured images to another by the satellites is dependent to time of acquisition and spectral signature including wavelength width, pixel depth and the resolution (N. Mishra et al., 2014) The dependent parameters to the satellite imagery requires an atmospheric correction algorithm, sun angle or illumination geometry and the associated properties to obtain ground reflectance determination (C. B. Schaaf et al., 2002). To define the ground reflectance, the historical of archived data scenes are impractical to obtain such parameters. The one alternative to define the intrinsic of radiometric information is to apply relative radiometric normalization (M. J. Canty, 2004). This method is an alternative even if the absolute surface reflectance is incapable to observe.

Commonly, relative radiometric normalization (RRN) is performed based on the assumption that the relationship between at-sensor radiances required at different time from the area of constant reflectance is approximated by linear function (Y. Du, 2002). With this method, evaluation on human activity and influence on the land surface, studying land cover changes, monitoring water quality and air pollution are linearly achievable. For example, the most longest archival of satellite images is Landsat satellite that reach up to 50 years continuously. Moreover, in order to multi-temporal coverage and spatial resolution that appropriate to human activity, the essential thing on Landsat satellites are the radiometric calibration consistency and stability (N. Mishra et al., 2014). Therefore, this makes Landsat satellites become a successful program on the further unrestrained mission to land cover change and global climate change studies with particular treatment to maintain image data requirement.

The key to conduct RRN is based on the feature selection to select pseudo invariant feature between paired images on different time. The transformation of digital number is by treating as linear function that tied up to the reference. In this kind of feature selection, (Y. Du, 2002) and (C.-H. Lin, 2015) has conducted by using principal component analysis, and (M. J. Canty, 2008) by using multivariate alteration detection (MAD). These kind of PIFs selection is deal with the linearity relationship between image acquisition. Another, the new method developed by (M. A. Syariz, 2019) uses weighting regression for linear regression to be nonlinear regression. However, based on the different of the intrinsic of spectral signature and pixel depth storage, this method is incapable to deal with. Therefore, each of captured images to another should be treated as different variation that are commonly nonlinear. This approach is inevitable if the use of linear relationship is applied.

In the recently research conducted by (L. G. Denaro, 2018) the PIFs selection is done by the nonlinearity that use projection of the data to higher dimensional called as Kernel function. Therefore, this method is called as kernel multivariate alteration detection (KMAD). K-MAD maintains the PIFs by projecting the samples into the higher dimensional feature space and assume it as nonlinearity from the original feature space. In the practical, this method experienced the complexity such as storage complexity and time complexity. This means that the few of region of interest is implemented only to determine PIFs. Therefore, the combination of KCCA projected back to original feature space and find its maximum correlation is implemented to preserve the size complexity and time complexity.

2. METHODOLOGY

2.1. Pseudo-invariant Feature Selection

In order to retrieve the invariant pixels between images in difference dates, call date 1 and date 2 in bitemporal image, we suppose to form the integration between them to find optimum correlation to discriminate pseudo invariant features (PIFs). There are many methods to extract PIFs, in this paper we would like to use Hybrid Kernel Canonical Correlation Analysis with the use of Multivariate Alteration Selection (MAD) method to change detection. In case of using the data, in this paper we provide date 1 represented as X and date 2 represented as Y of Landsat Imagery namely Landsat 7 and Landsat 8 respectively. Image X and image Y have p and q of bands respectively and each band has the same n pixel numbers. To make the matrices, we assume X and Y are pair of multiple vectors. Therefore, X and Y have numbers of vector bands respectively as shown below.

$$\mathbf{X}_{pxn} = \begin{bmatrix} X_{11} & X_{11} & \dots & X_{1n} \\ X_{21} & X_{21} & \dots & X_{2n} \\ \dots & \dots & \dots \\ X_{p1} & X_{p2} & \dots & X_{pn} \end{bmatrix} \mathbf{Y}_{qxn} = \begin{bmatrix} Y_{11} & Y_{11} & \dots & Y_{1n} \\ Y_{21} & Y_{21} & \dots & Y_{2n} \\ \dots & \dots & \dots \\ Y_{q1} & Y_{p2} & \dots & Y_{qn} \end{bmatrix} \tag{1}$$

Then, require the mean of each rows of $\mathbf{X}$ and $\mathbf{Y}$ images vectors called $E(\mathbf{X}_p)$ and $E(\mathbf{Y}_p)$ respectively. From the both mean variables mentioned, we retrieve the variance and covariance matrix vectors and generate correlation function subject to its variance (2).

$$\boldsymbol{\rho} = \frac{Cov(\mathbf{U},\mathbf{V})}{\sqrt{Var(\mathbf{U})xVar(\mathbf{V})}} = \frac{\mathbf{a}^T\sum_{XY}\mathbf{b}}{\sqrt{\mathbf{a}^T\sum_{XX}\mathbf{a}\mathbf{b}^T\sum_{YY}\mathbf{b}}} \tag{2}$$

By using Lagrange multiplier, this leads to the set of eigenvalues and eigenvector.

$$\sum_{XY}\sum_{YY}^{-1}\sum_{YX}\mathbf{a} = \rho^2\sum_{XX}\mathbf{a} \quad \sum_{YX}\sum_{XX}^{-1}\sum_{XY}\mathbf{b} = \rho^2\sum_{YY}\mathbf{b} \tag{3}$$

where $\mathbf{a}$, $\mathbf{b}$ and $\boldsymbol{\rho}$ is the linear factor namely eigen vector $\mathbf{a}$, $\mathbf{b}$ and corresponding eigen value $\boldsymbol{\rho}$. The equation above, then back to the projection that $\mathbf{U}_{pxn} = \mathbf{a}_{pxp}^T\mathbf{X}_{pxn}$ and $\mathbf{V}_{pxn} = \mathbf{b}_{qxq}^T\mathbf{Y}_{qxn}$ define the rotation axis. Therefore, according to (L. G. Denaro, 2018) we retrieve the normalized MAD by using equation.

$$\sum_{i=1}^{p}\left(\frac{MAD_i}{\rho_{MAD_i}}\right)^2 < threshold \tag{4}$$

where the decision threshold (*t*) is based on *chi-square* test. this threshold defines that if the values are smaller, the values could be called as no-change. The choosing threshold is under assumption that $\alpha = 0.05$ of probable observed. Subsequently, the sum of the mad square divided by standard deviation square refers to the degree of freedom *p*.

The algorithm discussed before is CCA-based MAD method that is the basic concept of change detection done in the original feature space. This method deals with the linear assumption of the reflectance and homogeneous. However, to encounter the radiometric difference of images which is in different sensor and atmospheric condition that has been discussed in Chapter 1, that linear based approach should be considered changes to the nonlinear approach and take into account (L. G. Denaro, 2018). Taking its projection of its nonlinear correlation on the higher dimensional feature space down into original space is the advanced concept to compensate nonlinearity problem in image processing. Therefore, this method is called as Hybrid-kernel CCA (HCCA) as shown in Figure 1. Such problem appears to be impractical hence concluded into two categories, storage complexity and time complexity detailed in Table 1 and Table 2 respectively.

Table 1. Storage complexity

Image size	KCCA (Memory capacity)	HCCA (Memory capacity)
50 x 50	5.71 GB	5.54 GB
100 x 100	8.84 GB	5.55 GB
120 x 120	8.95 GB	5.57 GB
150 x 150	35.1 GB	5.61 GB
200 x 200	114.3 GB	5.65 GB
300 x 300	~	6.04 GB

Table 2. Time complexity

Image size	KCCA	HCCA
50 X 50	28 seconds	0.05 Seconds
100 X 100	15 Minutes	0.26 Seconds
120 X 120	41 Hours	0.51 Seconds
150 X 150	2.8 Hours	1.6 Seconds
200 X 200	49 Hours	7.9 Seconds
300 X 300	~	1 Minutes

Finally, by using HCCA the values that are lower to the threshold or called as invariant pixels between two date of images, will be conducted regression process as the further step. In this paper, there are three comparable regressions used namely linear regression, non-linear regression and proposed Gaussian weighting regression that will be explained in the following section.
One of the idea to Figure 1 is to adjust the regularity of different pixels to be uniform or turn it to be equivalent level that come from different spectral signatures.
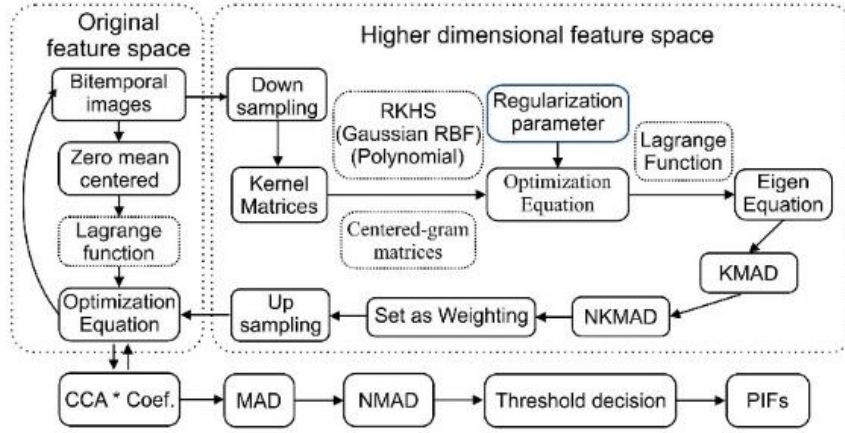
Figure 1. Flowchart of Hybrid-CCA

2.2. Linear and nonlinear regression

To define the parameters that generate the normalized image, the key to do is to use selectable or acceptable PIFs. These selected PIFs have been done in the previous chapter. The least square regression used to develop fitting line between two images, PIFs of Landsat 7 and Landsat 8. The two methods use polynomial regression from degree 1 to degree 5 as shown in Figure 2 (left), and power-law regression from degree 0.1 to degree 1.5 as shown in Figure 2 (right). The linear regression is stated in Figure 2 for degree 1. We can see that there are having particular characteristic of fitting line motion or curve. For the polynomial regression, the curve-lines are problematic in the mapping function to *y-value axis*. For example, the problematic mapping functions appear merely visible to degree 3 to degree 5. However, the degree 2 also involves in the higher gray level values. Therefore, only linear fitting line is acceptable to conduct mapping function.

The idea to power-law mapping function is to transform with respect to the term of monotonically increasing function. This term is precondition in digital image mapping which can be calculated inversely without redundant. In Figure 2 (right), degree 0.1 to degree 1.5 are fulfilling prerequisite mapping function.

Therefore, this strategy to transform the digital image tied up to the reference is believable and become major discussion with recombination to Gaussian distribution function as proposed method. This Gaussian function is set to be weighting that bound to linear and nonlinear function. There are two condition to determine the standard deviation σ based on the mean μ as explained in equation (5). x is gray value digital number.

$$f(x,\sigma,\mu) = \begin{cases} e^{\frac{-(x-\mu)^2}{2\sigma^2}} & , \ x < \mu \\ e^{\frac{-(x-\mu)^2}{2(3\sigma)^2}} & , \ x \geq \mu \end{cases} \tag{5}$$
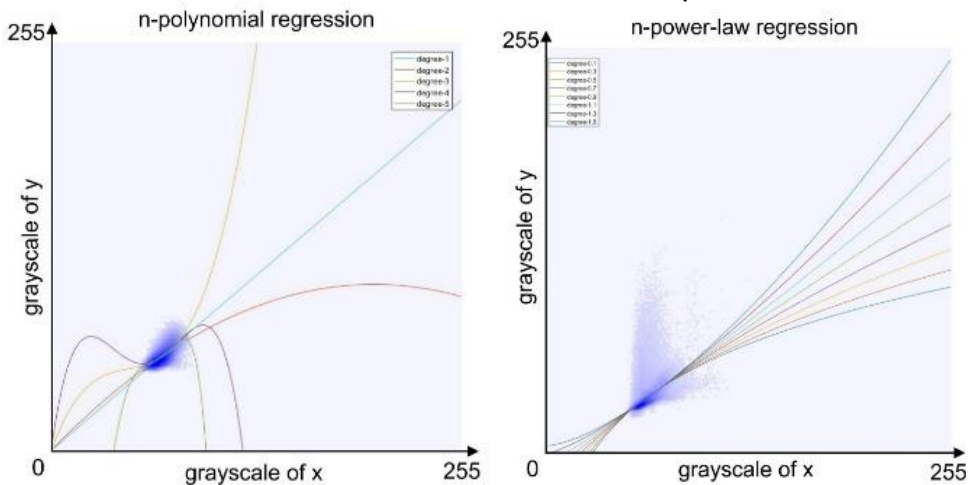
Figure 2. Polynomial least square regression (left) and Power-law least square regression (right)

To better understanding in equation (5), it can be clearly depicted in Figure 4 about how to determine the Gaussian weighting distribution function.
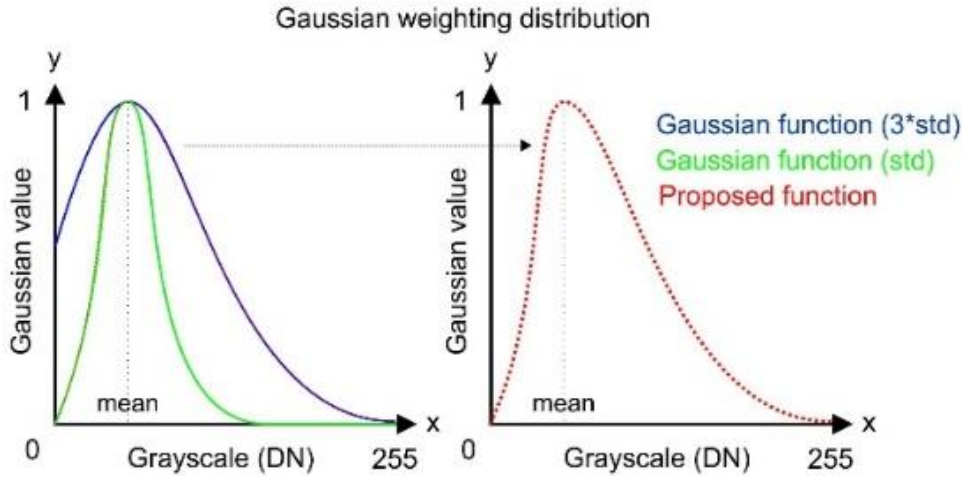
Figure 3. Proposed Gaussian weighting function

2.3. Normalization technique

Normalization technique is the last step of image transformation. The image that need to be transformed is at the first time treated as dependent variable. In this case, Landsat 8 imagery is going to be transformed to Landsat 7 radiometric level (common level). To be concluded, Figure 4 is an illustration and it is denoted by the formula in equation (6).
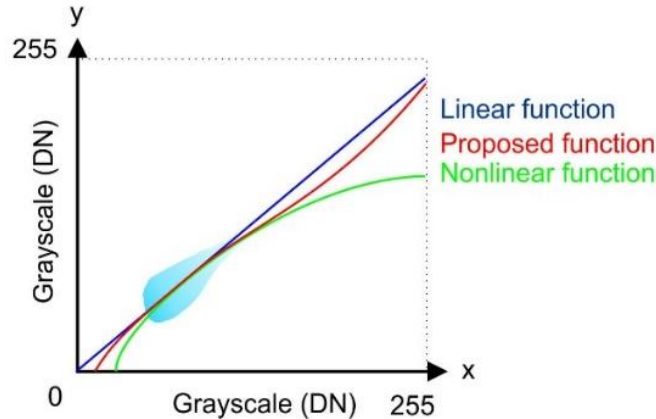
Figure 4. Proposed normalization function (monotonically increasing)

$$\overline{Y} = f(x, \sigma, \mu) * R_1(x) + \big(1 - f(x, \sigma, \mu)\big) * R_2(x) (6)$$

R_1 and R_2 are the linear and nonlinear of regression function.

3. STUDY AREA

Landsat data of Taiwan and Japan region for 2013 to 2017 were used in this research. There are two datasets at different sensor of each location, namely Landsat 7 ETM+ and Landsat 8 OLI. Landsat 7 images were selected as the reference image.

4. RESULT AND DISCUSSION

This section describes the visual and statistical result from three different RRN methods. The visual result is determined by comparing of normalized data images by the display and judge the overall performance of these methods. Both of radiometrically normalized images and reference images are displayed side by side on the monitor screen, and the visual closeness of each normalized image to the reference image is determined by qualitatively. If the visual image of the subject changes approaching to the reference and become similar or identical based on radiometric level, the image

can be regarded as radiometric adjusted to the reference image as shown in Figure 5. However, this visual comparison method has less convinced since our visual is prone to subjectivity. Therefore, a quantitative comparison will be discussed in the following section.

Figure 5. Mosaic images of Landsat 7 (up) and Landsat 8 (down) of normalized images (Japan region)

4.1. Root mean square error (RMSE)

In quantitative comparison, we apply RMSE. RMS error is used to measure the statistical agreement of normalized image with the reference image.

Table 3. Normalized images: Root mean square error (RMSE)

Band	Taiwan (RMSE)			Japan (RMSE)		
	LN	NL	PM	LN	NL	PM
1	1.23	1.26	**1.26**	1.82	1.80	**1.80**
2	1.08	1.16	**1.16**	2.03	2.03	**2.00**
3	1.29	1.42	**1.41**	2.33	2.36	**2.35**
4	2.29	7.02	**6.64**	4.07	6.65	**6.25**
5	2.34	6.69	**6.41**	3.32	6.11	**6.00**
6	1.48	2.89	**2.8**	2.33	3.38	**3.33**

You can see the algorithm in the equation 7 as follows.

$$RMSE_p = \sqrt{\frac{\sum_1^n (DN'_{est} - DN_{ref})^2}{n}} \tag{7}$$

where DN'_{est} represents the normalized digital number of band p of Landsat 8 imagery, DN_{ref} is the digital number of band q in reference image.

Thus, the digital number of pixels of the normalized image are compared with those of reference image of the corresponding band. If the difference between these number is quite small, the RMSE result will be small, this is implying that the Landsat 8 imagery is radiometrically more similar to the reference image. The result of RMSE as follows on Table 3.

5. CONCLUSION

This study presents a HCCA based PIF extraction and Gaussian weighting regression on the Landsat 7 and Landsat 8 imagery. The proposed PIFs extraction method result regularity of different pixels to be uniform or turn it to be equivalent level that come from different spectral signatures and this equivalent radiometric level furthermore to be the object of PIFs extraction based on heterogeneous spectral dependency. To treat the heterogeneous pixel signatures, the proposed normalization procedure is then applied. This kind of procedure become more flexible in the relative radiometric normalization.

REFERENCE

D. Yuan and C. D. Elvidge, "Comparison of relative radiometric normalization techniques," ISPRS J. Photogramm. Remote Sens., vol. 51, no. 3, pp. 117–126, 1996.

N. Mishra, M. O. Haque, L. Leigh, D. Aaron, D. Helder, and B. Markham, "Radiometric cross calibration of landsat 8 Operational Land Imager (OLI) and landsat 7 enhanced thematic mapper plus (ETM+)," Remote Sens., vol. 6, no. 12, pp. 12619–12638, 2014.

C. B. Schaaf et al., "First operational BRDF, albedo nadir reflectance products from MODIS," Remote Sens. Environ., vol. 83, no. 1–2, pp. 135–148, 2002.

M. J. Canty, A. A. Nielsen, and M. Schmidt, "Automatic radiometric normalization of multitemporal satellite imagery," Remote Sens. Environ., vol. 91, no. 3–4, pp. 441–451, 2004.

Y. Du, P. M. Teillet, and J. Cihlar, "Radiometric normalization of multitemporal high-resolution satellite images with quality control for land cover change detection," Remote Sens. Environ., vol. 82, no. 1, pp. 123–134, 2002.

C.-H. Lin, B.-Y. Lin, K.-Y. Lee, and Y.-C. Chen, "Radiometric normalization and cloud detection of optical satellite images using invariant pixels," ISPRS J. Photogramm. Remote Sens., vol. 106, pp. 107–117, 2015.

M. J. Canty and A. A. Nielsen, "Automatic radiometric normalization of multitemporal satellite imagery with the iteratively re-weighted MAD transformation," Remote Sens. Environ., vol. 112, no. 3, pp. 1025–1036, 2008.

M. A. Syariz, B. Y. Lin, L. G. Denaro, L. M. Jaelani, M. Van Nguyen, and C. H. Lin, "Spectral-consistent relative radiometric normalization for multitemporal Landsat 8 imagery," ISPRS J. Photogramm. Remote Sens., vol. 147, no. March 2018, pp. 56–64, 2019.

L. G. Denaro, L. Bo-Yi, M. A. Syariz, L. M. Jaelani, and C.-H. Lin, "Pseudoinvariant feature selection for cross-sensor optical satellite images," J. Appl. Remote Sens., vol. 11, no. 1, 2018